Real-time Tracking of Proton Transfer from the Reactive Cysteine to the Flavin Chromophore of a photosensing Light Oxygen Voltage protein

Raiza N. A. Maia[1], David Ehrenberg[1], Sabine Oldemeyer[1], Esther Knieps-Grünhagen[2], Ulrich Krauss[3], Joachim Heberle[1,*]

[1] Freie Universität Berlin, Department of Physics, Experimental Molecular Biophysics, Arnimallee 14, 14195 Berlin, Germany;

[2] Institut für Molekulare Enzymtechnologie, Heinrich-Heine-Universität Düsseldorf, Forschungszentrum Jülich, D-52426 Jülich, Germany

[3] Institute of Bio- and Geosciences (IBG-1): Biotechnology, Forschungszentrum Jülich, D-52426 Jülich, Germany

KEYWORDS. FTIR; blue-light photoreceptor; bacteriorhodopsin; time-resolved IR spectroscopy; quantum cascade laser

LOV (Light Oxygen Voltage) proteins are photosensors ubiquitous to all domains of life. A variant of the short LOV protein from *Dinoroseobacter shibae* (DsLOV) exhibits an exceptionally fast photocycle. We performed time-resolved molecular spectroscopy on DsLOV-M49S and characterized the formation of the thio-adduct state with a covalent bond between the reactive cysteine (C72) and C_{4a} of the FMN. Using a tunable quantum cascade laser, the weak absorption change of the vibrational band of S-H stretching vibration of C57 was resolved with a time resolution of 10 ns. Deprotonation of C72 proceeded with a time constant of 12 µs which tallies the rise of the thio-adduct state. These results provide valuable information for the mechanistic interpretation of light-induced structural changes in LOV domains, which involves the choreographed sequence of proton transfers, changes in electron density distributions, spin alterations of the latter, transient bond formation and breakage. Such molecular insight will help developing new optogenetic tools based on flavin photoreceptors.

Blue-light photoreceptors are widely found in all kingdoms of life where they regulate different cellular functions such as phototropism, chloroplast movement and stomatal opening [1-3]. Characteristic to this family of photoreceptors is the chromophoric cofactor flavin, which gives rise to the yellow color with a maximum absorption at around 450 nm. Cryptochromes (CRYs) and BLUF photoreceptors (blue-light sensors using flavin) carry flavin adenine dinucleotide (FAD) as a cofactor whereas the majority of LOV photoreceptors (light, oxygen, voltage) harbor a flavin mononucleotide (FMN). These blue-light receptors extend the toolbox of optogenetics beyond the prominent rhodopsins [4].

LOV domains undergo cyclic photoreactions that are initiated in the femto- to picosecond time range by excitation of the FMN cofactor into the excited singlet state [5-6]. Efficient intersystem crossing (ISC) populates the triplet state ($[LOV]^3$) on the nanosecond time scale [7-8]. In the subsequent microsecond time range, a small fraction of the triplet state decays back to the ground state, while the majority of the molecules yield a covalent FMN-cysteinyl-thiol-adduct ($[LOV]^A$ – Figure 1A). This adduct is formed between the FMN chromophore and the terminal thiol group of a nearby cysteine residue, involving the deprotonation of the thiol moiety (Figure 1A), as observed in the LOV domain from *Chlamydomonas reinhardtii* [9]. Interestingly, in *Chlamydomonas* LOV2 the covalent adduction formation was found to also occur from the singlet state as reported by Zhu et. al.[10]. The proton of the cysteine is released, the N_5 atom of the FMN gets protonated and a covalent bond is formed between the cysteine residue and the C_{4a} atom of the FMN isoalloxazine ring (Fig. 1A and [11-16]). It is well accepted that the adduct state represents the active signaling state of LOV domains [17-18] not just due to its long-lived nature but also because other intermediates have not been observed between the decay of $[LOV]^A$ and the recovery of the initial ground state. Finally, the photocycle is completed when $[LOV]^A$ reverts spontaneously back to its original dark state in a few seconds to hours [5, 7-8, 16, 19-22].

Despite extensive research into the photoreaction of LOV domains over the last two decades, the reaction sequence leading to the formation of the flavin-cysteine adduct has not yet been resolved. Various scenarios have been proposed [7-8, 13-15, 23-24] out of which a radical pair mechanism is currently favored. Here, the adduct state is formed by electron transfer or movement of a hydrogen atom from the reactive cysteine (C72) to the N_5 atom of the FMN followed by ISC back to the singlet state and finally bond formation between C_{4a} of FMN and the side chain of the cysteine [13].

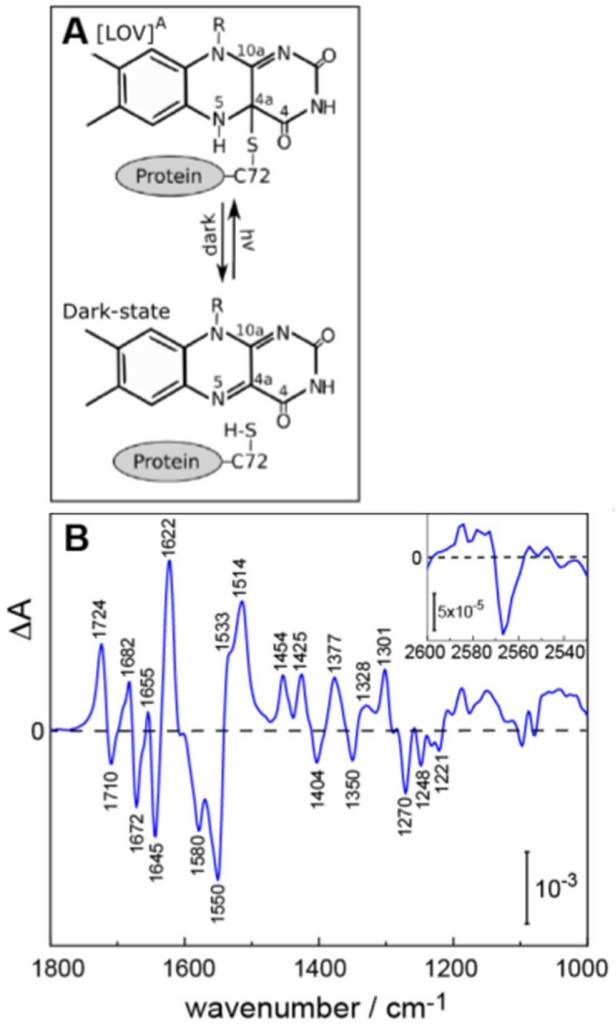

Still, the time scale of proton transfer from the cysteine to N_5 of FMN has not been determined yet.

Figure 1 (A) Chemical structure of the catalytic co-factor FMN in LOV domains. Blue light excitation induces the reversible formation of the covalent bond between FMN and the C72 residue. The adduct ($[LOV]^A$) reverts spontaneously back to the dark state on a timescale of seconds to hours. (B) Light-induced FTIR difference spectrum of DsLOV-M49S from 1800 – 1000 cm^{-1}. The inset depicts the spectral range of the S-H stretching vibration from 2600 – 2500 cm^{-1}. The indicated frequencies are compiled and assigned in Table S1.

In this report, we present time-resolved IR experiments on the short LOV protein DsLOV from the photoheterotrophic marine α-protobacterium *Dinoroseabacter shibae*. The protein, which has no fused effector domain [25-29], was only recently described and characterized with regard to structure and function [30-31]. Strikingly, DsLOV exhibits unique characteristics opposed to other LOV photoreceptors as it was found to participate in the regulation of photopigment synthesis in the absence of blue light. To this end, the dark state is the physiologically relevant signaling state. DsLOV exhibits an accelerated photocycle with a lifetime of the adduct state of τ = 9.6 s[30]. DsLOV carries a methionine residue at position 49 [30-31], where isoleucine or leucine residues are found at this position in other LOV domains. Several studies have shown that the exchange of this residue strongly influences the lifetime of the adduct state of LOV proteins [7, 21, 31]. Replacement of M49 by serine in DsLOV produces a variant with a faster dark-state recovery in the absence of large structural alterations compared to the wild type [31]. The accelerated recovery rate of dark-state DsLOV-M49S after photoactivation (τ = 1.6 s [31]) facilitates time-resolved IR spectroscopic experiments to study the mechanistic details of the photoreaction of LOV proteins.

Dark-state DsLOV-M49S exhibits the vibrationally fine structured electronic absorption with maximum at around 450 nm that is characteristic to flavoproteins. Formation of the cysteinyl adduct is accompanied by changes in the vibrational modes of the FMN cofactor and the apoprotein as recorded by FTIR difference spectroscopy (Figure 1B). Here, negative bands represent vibrations due to the dark state of the protein, whereas positive bands arise from contributions of the adduct state. In this frequency range, the spectrum is dominated by changes in the vibrational bands of the FMN chromophore because formation of the cysteinyl-adduct state induces large changes in the dipole moment of FMN [32]. The agreement between the DsLOV-M49S and spectra of other LOV domains [12, 32-33] permits the assignment of vibrational bands (Table S1). The C_4=O vibrational mode is of particular interest due to its sensitivity not just to the triplet state but also to adduct-state formation. Its frequency shifts from 1710 cm^{-1} in the dark state to 1724 cm^{-1} upon formation of the covalent bond to the cysteine [29, 32, 34-35]. The 1533 cm^{-1} vibrational mode is a direct proxy to track the formation of the adduct state. This band undergoes major changes during the transition of the C_{4a} carbon from a planar carbon (sp^2) to a non-planar tetrahedral carbon (sp^3) in the C_{4a}–N_5 single bond upon adduct formation [29, 36]. Unlike other LOV domains, DsLOV-M49S does not show strong amide-I bands after covalent bond formation [29, 32, 34-35] which may be related to the absence of the Jα helix in the protein structure [30-31], which gives rise to absorption changes in the amide I range after [LOV]A formation in other LOV domains [37].

Given that steady-state experiments do not provide any information on the time scale of the light-induced changes, we performed time-resolved IR experiments using a flash photolysis spectrometer employing the intense emission from a tunable external cavity quantum cascade lasers (EC-QCLs). The high photon flux of QCLs [38] facilitates the detection of contributions of single amino acids such as the weak S-H vibration of a cysteine residue (see inset of Fig. 1B). Detection of this vibrational band is hampered by the low extinction coefficient, ranging from ε = 10-200 $M^{-1}cm^{-1}$ depending on the hydrogen-bonding properties of the solvent [38 39]. Our QCL experiments cover the spectral range from 2600-2520 cm^{-1} and from 1800-1510 cm^{-1} resolving the signature modes of the S-H stretching vibration as well as the amide I (mainly C=O) mode of the peptide backbone, and the C=O and C=N stretching vibrations of FMN, respectively. Time-resolved IR data were recorded over the range of 50 ns – 500 ms. To correlate the vibrational changes with the electronic alterations in the FMN chromophore, we also recorded time-resolved UV/Vis absorption changes in the range from 380 - 720 nm over a time range of 50 ns - 10 s.

Covalently linking C72 to the C_{4a} of FMN requires prior deprotonation of the terminal thiol moiety of the cysteine side chain. The deprotonation appears in the light-induced difference spectrum as a negative band at 2566 cm^{-1}, a typical frequency of the S-H stretching vibration of cysteines (inset Figure 1B) [39]. Consequently, we assign this negative band to the deprotonation of C72, the only cysteinyl residue of DsLOV. The frequency of the S-H stretch of the C72 in DsLOV-M49S in the steady-state experiment is in the same range as reported for other LOV domains [12, 32-33, 40].

Using an EC-QCL, we track the minute absorbance changes of the S-H vibration of DsLOV-M49S (Figure 2). The observed minimum at 2566 cm^{-1} exactly matches the frequency of the S-H vibrational band as determined by steady-state FTIR difference spectroscopy (Figure 1B). The temporal evolution of the S-H vibration is overlapped by broad IR absorption changes caused by heat transfer from the photoexcited protein to the surrounding aqueous medium (Figure 2A). To separate the kinetics of the band at 2566 cm^{-1} from the heat-induced changes, we integrated the absorption changes across the range of 2550-2520 cm^{-1} and subtracted this time trace from the kinetic at 2566 cm^{-1} (see Figure S3). The time trace (Figure 2B) exhibits the rise of the bleach with a time constant of τ = 12 µs, corresponding to the time constant of deprotonation of the reactive cysteine residue C72.

The question emerges from these results if proton transfer from C72 to FMN is rate-limiting to the succeeding reactions? Therefore, we conducted time-resolved UV/Vis spectroscopy to track electronic changes of the FMN chromophore. The triplet state formed in LOV domains has characteristic absorption bands in the UV/Vis at 390, 660 and 720 nm [8, 14-16]. Figure 3A depicts an exemplary decay of

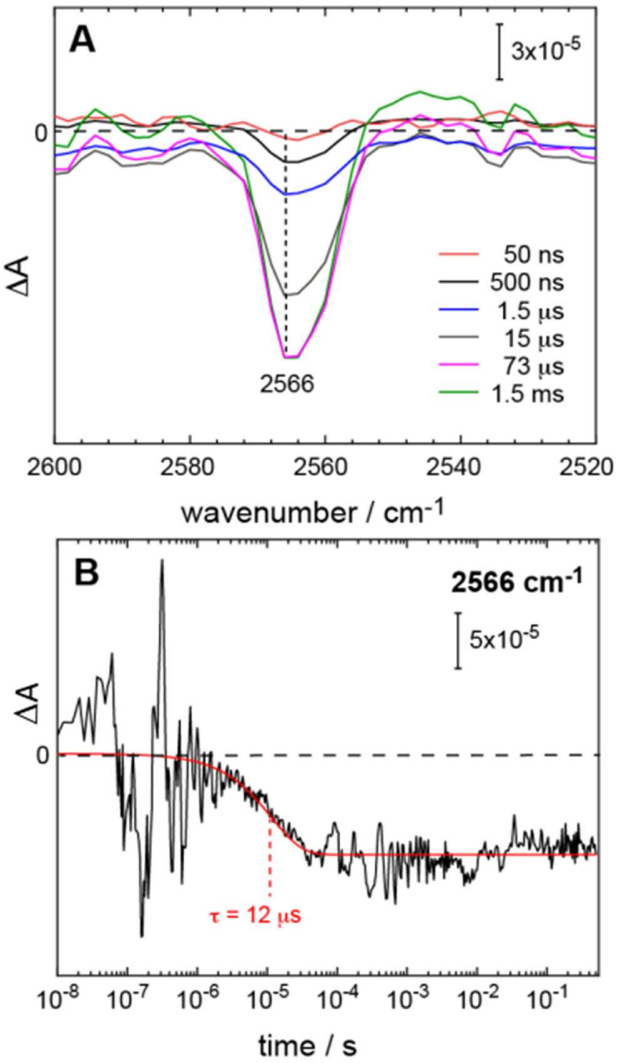

Figure 2 (A) IR difference spectra of the temporal depletion of the vibrational band of the S-H stretching vibration of C72 of DsLOV-M49S due to deprotonation of C72. Data have been recorded by time-resolved flash photolysis using a tunable EC-QCL. **(B)** The initial absorption at 2566 cm^{-1} decays mono-exponentially into a plateau (black trace) with a time constant of 12 µs (red trace).

the triplet state recorded at 660 nm. Traces have been fitted by global analysis (Figure 3) and the derived time constants are summarized in Table 1. The triplet state decays with two time constants (τ_1 = 13 µs and τ_2 = 215 µs) in the visible range. The triplet decay is corroborated by the kinetics of the vibrational changes recorded at 1654 cm^{-1} which proceed with a similar time course (τ_1 = 18 µs and τ_2 = 101 µs) supporting not only the assignment to the C_4=O vibration in the triplet state but also the biexponential decay [5]. As both the adduct and the triplet state, absorb at 390 nm, the kinetics (Figure 3B) shows two clearly separated decay components with τ_1 = 13 µs and τ_3 = 0.53 s. The former reflects triplet decay and the latter of the adduct state. In

the adduct state $[LOV]^A$ (Figure 1, Table S1), the C_4=O vibration absorbs at 1726 cm^{-1} [29, 32, 34, 36] and the rises with the same time constant as the triplet decay, indicating the absence of any other (observable) intermediate states in between.

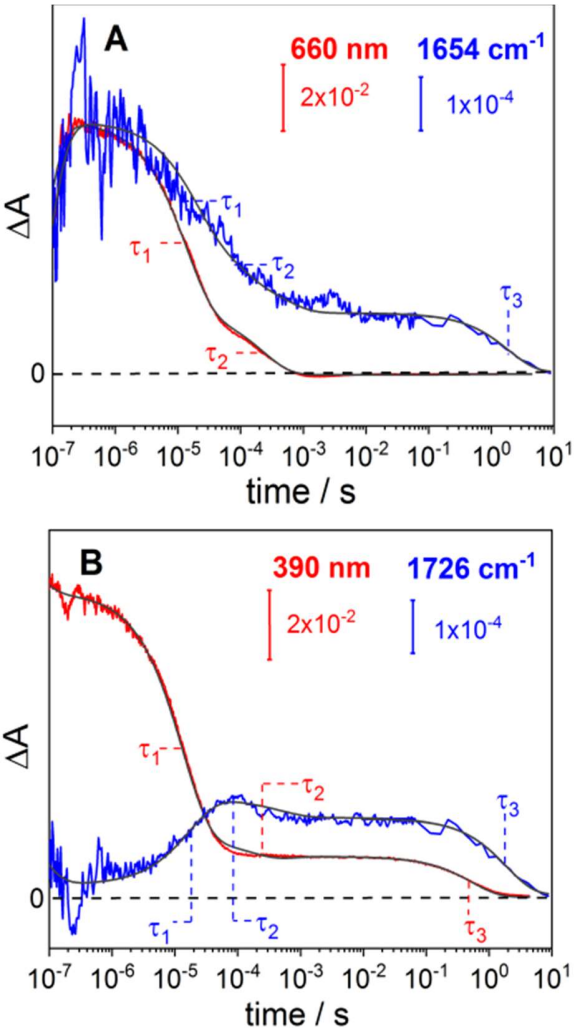

Figure 3 Selected kinetics of vibrational bands from time-resolved IR (blue) and UV/Vis (red) absorption experiments. The recorded kinetics were subjected to global fitting (grey smooth lines) and the derived time constants are displayed in Table 1. (A) The kinetics at 660 nm reflect the decay of the triplet state ($[LOV]^3$). The vibrational mode at 1654 cm^{-1} is due to the C_4=O vibration of the triplet state. (B) The early absorption changes at 390 nm refer to the decay of the triplet state and the formation of the adduct state, as both intermediate species exhibit electronic absorption at this wavelength. The IR kinetics at 1726 cm^{-1} tally formation of the adduct state.

We analyzed the time-resolved IR and UV/Vis datasets (Figure S4) by global fitting and applied a photocycle model with branched triplet decay in the absence of a (observable) radical state (Figure 4). This reaction scheme was selected based on lifetime density analysis and testing of other models by global analysis (Figures S6 and S7). Gil et al. [5] were able to fit time-resolved infrared data with a branched triplet decay but excluded the model due to a discrepancy between a short decay of the triplet back to the ground state and a long-lived triplet upon mutation of the cysteine to a valine [5]. In our case, the triplet decay to the ground state is in agreement for an unquenched triplet state. Contrary, Kutta et al. favored the decay of the radical anion intermediate back to the ground state with the same 4:1 ratio after a thorough analysis of their UV/Vis data [9]. The concurrent decay of the triplet state back to the original dark state without formation of the adduct state could indicate the presence of a cysteine rotamer as observed in crystal structures of LOV domains from *Chlamydomonas reinhardtii* and *Avena sativa* [12, 14, 37]. Although the crystal structures of DsLOV and DsLOV-M49S did not reveal different rotamers, the cysteine side chain can adopt two different conformations in the WT and M49S [30-31]. It is noted that the two rotamers can interconvert on the nanosecond timescale as shown by MD simulations on the *Avena sativa* phototropin 1 LOV2 (AsLOV2). Here, the reactive cysteine residue was flipping rapidly from one conformer to the other, presenting a dynamic equilibrium. [41] Consequently, it seems unclear if the rotamers in DsLOV would be more stable. However, our data indicate the presence of two rotamers, given the asymmetric shape of the SH band. Fitting two Gaussians to the asymmetric shape of the S-H stretching band provided two minima at 2566 cm^{-1} and 2560 cm^{-1} (Figure S2B) indicating that C72 adopts two different rotamer orientations in dark-state DsLOV-M49S under our ambient conditions. The relative area of each vibrational band is 67% and 33%, respectively, which is very similar to LOV1 from *Chlamydomonas reinhardtii* [12].

Based on this model, we have derived species associated spectra (SAS) from our photocycle model (Figure 5) that refer to the IR difference spectra of the intermediate states. The spectrum in black corresponds to the triplet state of DsLOV-M49S [5, 11, 42-43] which is formed beyond our time resolution. The most prominent negative band at 1548 cm^{-1} and the negative band at 1580 cm^{-1} are due to coupled C=N and C=C stretching vibrations of the isoalloxazine ring of FMN in the dark state [5, 44]. The former vibrational band appears downshifted by 4 cm^{-1} in comparison with the LOV1 and LOV2 from *Chlamydomonas reinhardtii* and the LOV domain of *Bacillus subtilis* [12]. The negative band at 1676 cm^{-1}, assigned to the C_2=O stretching vibration, exactly matches the frequency in other LOV domains [12]. The shift of the C_2=O stretching vibrations at 1676(-)/1624(+) together with the positive band at 1654 cm^{-1} are assigned to the carbonyl vibrations in the (deprotonated) triplet state [5, 11, 36, 42-44]. Global fitting shows that the triplet state decays with τ_1 = 18 µs. With the rise of the adduct state, two new positive bands appear at ~1684 cm^{-1} and at 1726 cm^{-1}, the latter is due to the upshift of 1710(-) cm^{-1} vibrational mode

(Figure 5 - red spectrum). The 1726(+) cm^{-1} vibrational mode was assigned to the C_4=O stretching vibration which indirectly indicates formation of the adduct state [6, 42]. The 1538 cm^{-1} band would be the direct proxy to track the adduct state formation, given that this mode arises upon the disappearance of the C_{4a}=N_5 double bond and formation of the C_{4a}–N_5 single bond [2, 5]. Although the vibrational band appears only as a shoulder at 1538 cm^{-1} (Fig. 5), the kinetics of adduct formation as evidenced by the rise of the bands at 1726 cm^{-1} (blue trace in Fig. 3B) and at 1538 cm^{-1} coincides with the deprotonation of C72 as derived from the S-H vibrational band at 2566 cm^{-1} (Fig. S8).[1].

Table 1 Time constants of the DsLOV-M49S photoreaction derived from global analysis of time-resolved spectroscopy. The model includes a branching of the triplet decay to either direct restoration of the dark state or formation of the cysteinyl adduct.

τ (s) of intermediate state transitions	1800 – 1510 cm^{-1}	730-380 nm
τ_1 ($[LOV]^3 \rightarrow [LOV]^A$)	18 µs	13 µs
τ_2 ($[LOV]^3 \rightarrow [LOV]^1$)	83 µs	196 µs
τ_3 ($[LOV]^A$)	510 µs	--
τ_4 ($[LOV]^A \rightarrow [LOV]^1$)	1.9 s	0.56 s

According to the characteristic marker bands observed in the spectra, formation of a protonated triplet state can be excluded. The protonated $[LOV]^3$ typically shows three vibrational modes for the C=O vibrations instead of the observed two bands at 1654 cm^{-1} and 1624 cm^{-1} of the neutral $[LOV]^3$ [11, 43]. Although no intermediate states were observed between triplet decay and adduct state formation, transient formation of either the flavin neutral radical ($FMN^{\bullet}$) or the flavin anion radical ($FMN^{\bullet-}$) cannot be strictly excluded. Both species have been characterized spectroscopically in solution. The anion radical generated by the photoreduction of FMN by ethylenediaminetetra-acetic acid disodium salt dihydrate (EDTA) shows a prominent band at 1633 cm^{-1} [43], which slightly shifts to 1636 cm^{-1} due to solvent effects if $FMN^{\bullet-}$ is generated using riboflavin tetraacetate (RBTA) in CD_3CN [42]. The spectrum of the neutral radical generated by RBTA in CD_3CN has marker bands at 1660 cm^{-1} and 1620 cm^{-1} [42] close to the band positions detected in our data at 1654 cm^{-1} and 1624 cm^{-1} and are, thus, possibly concealed by triplet vibrations. However, it may well be that these states are not sufficiently populated to be monitored in our time-resolved experiments.

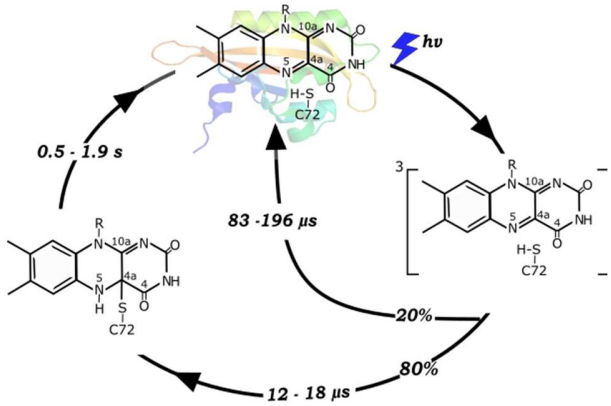

Figure 4 Scheme of the suggested photocycle of DsLOV-M49S initiated upon blue-light illumination. Time constants are derived from global analysis of time-resolved experimental data in the IR and UV/Vis region (Table 1). After light excitation, the DsLOV-M49S relaxes to a triplet state $[LOV]^3$ where a small fraction (20%) is not forming the adduct state but decays back to the dark state. The fraction that passes the triplet state (80%) decays via a concerted mechanism or via formation of a triplet radical state to form the adduct state $[LOV]^A$. At last the adduct state decay back to the ground state in a time range between 0.5 and 2 s.

We also observe the fast recovery of the bands at 1580 and 1548 cm^{-1} in the third SAS (blue spectrum in Figure 5) while the bands in the 1730-1600 cm^{-1} range remain practically constant, a phenomenon which was not observed in other LOV domains[44]. The deviation in the 1730-1600 cm^{-1} range could be due to the unique structural characteristics and function of DsLOV-M49S. MD simulations[45] pointed out the functional differences between LOV1 and LOV2. Whereas the LOV1 activation is mostly caused by changes in the hydrogen bonding between protein and ligand, LOV2 activation could also result from a change in the flexibility of a set of protein loops. The crystal structure of wild-type DsLOV shows a unique structural feature as the N-terminal A′α helix is part of the dimer interface[30]. An increased flexibility of the N-cap region was inferred from CD spectroscopy which could result in unfolding of the A′α helix in solution [31]. Similar structural changes have been reported for AsLOV2 [46], including side-chain displacements and changes in hydrogen-bonding patterns in the chromophore binding pocket and the amino-terminus. These rearrangements are interpreted as a starting point for changes in the A′α helix, which would contribute to the starting of the unfolding of the J-alpha helix [36]. Since DsLOV does not have a J-alpha helix, changes in the range from 1730 to 1600 cm^{-1} would be smaller or non-existing in comparison to other LOV domains that have a J-alpha helix [30-31].

Swartz et. al.[29] suggested that the bands at (-)1580/(-)1548 cm^{-1} originate from the C_{4a}=N_5 stretching vibration with a contribution of C_{10a}=N_1 in the (-)1580 cm^{-1} band. Thus, these two bands are expected to be strongly affected by the formation of the adduct state, due to the conversion of the C_{4a}=N_5 double bond to a C_{4a}-N_5 single bond upon formation of the adduct state [29]. The exchange of a planar carbon (sp^2 : C_{4a}=N_5) to a tetrahedral carbon (sp^3: C_{4a}-N_5) would justify the strong changes observed in the (-)1580/(-)1548 cm^{-1} vibrational modes (Figure 5).

As shown above, the time constants of the fast decay component of the triplet state obtained by global analysis $\tau_{UV/Vis}$ = 13 µs (Table 1- 730-380 nm) and τ_{IR} = 18 µs (Table 1- 1800-1514 cm^{-1}) are in good agreement with the time constant of the deprotonation of C72 (Figure 2A). Thus, we can infer that the formation of the C_{4a}-S bond and deprotonation of the cysteine residue run in concert, which probably is the rate-limiting step for the formation of the adduct state.

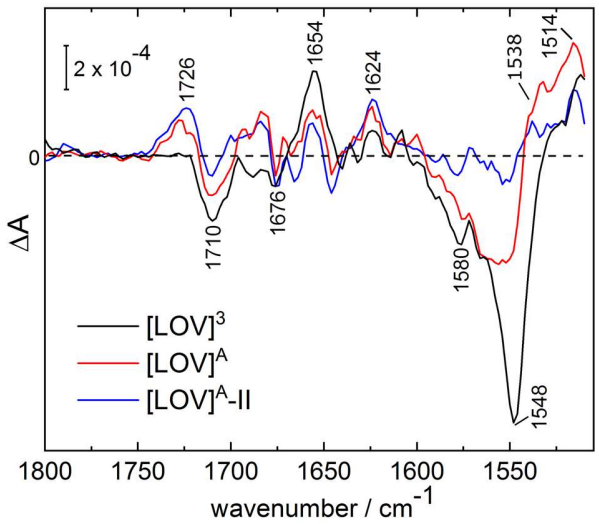

Figure 5 Species associated spectra (SAS) showing the key intermediate states of the DsLOV-M49S photoreaction recorded by time-resolved IR spectroscopy. Corresponding time constants are listed in table 1. The black spectrum corresponds to the vibrational changes of the dark state to the triplet state ($[LOV]^3$) and the red spectrum to the adduct state ($[LOV]^A$). The blue spectrum refers to the second adduct state ($[LOV]^A$-II), deviating from the first one mainly in the spectral range of 1580 - 1520 cm^{-1}.

Based on these results and the comparison to literature, a mechanistic model of the photocycle of DsLOV-M49S is presented in Figure 4.

With the time resolution of 50 ns of our setups for IR and UV/Vis spectroscopy, we were able to record the photoreaction of DsLOV-M49S starting from the triplet state. Various models have been suggested for the molecular mechanisms of covalent adduct formation in LOV domains [8, 11, 43, 47-48]. The radical-pair mechanism is well supported by experimental and computational models [13-14, 24, 47-51]. UV/Vis absorption spectroscopy, mass spectrometry and X-ray crystallography have been applied to investigate the neutral radical species produced by the cysteine variant of *Chlamydomonas* LOV1 [52]. The same flavin radical was directly identified by electron paramagnetic resonance (EPR) and characterized with electron nuclear double resonance (ENDOR) [53]. Besides these, evidence was found for the radical intermediate by investigating wild-type LOV1, LOV2 and cysteine mutants from *Chlamydomonas reinhardtii* [9]. The authors suggest the presence of a radical intermediate with a short lifetime in the wild type. These conclusions are in line with QM/MM simulations [13] which showed that the electron density at the N_5 atom increases during the $[LOV]^3$ transition, leading to a decrease in the N_5-C_{4a} double-bound character and to the formation of a neutral radical pair. The formation of a possible radical intermediate state generates an unpaired spin localized on the atoms involved in the adduct formation (Cys-S, FMN-C_{4a} and FMN-N_5) [13]. These conditions favor strong spin-orbit coupling constant, leading to efficient triplet-singlet ISC by the sulfur atom, resulting into a rapid decay of the radical intermediate state. Due to its short lifetime, the flavin radical state may not sufficiently populate to be detected in time-resolved experiments [35]. Another possibility is that a spectral contribution is obscured by the triplet signal as it is the case for the neutral radical with similar marker bands compared to neutral triplet state $[LOV]^3$ at 1660 cm^{-1} and 1620 cm^{-1} [42]. Although we do not clearly detect a radical species in our time-resolved data, we favor a radical-pair mechanism for DsLOV-M49S. In the ionic mechanism, a proton transfer from the cysteine to FMN results in a protonated triplet state [48]. This is in contrast to the triplet state detected in our experiment which was identified by two marker bands at 1654 cm^{-1} and 1624 cm^{-1} as unprotonated at N_5. It is also possible that the protonated triplet state is formed as a short lived intermediate not detectable in our experiments. However, Kay et. al. [49] argued that this ionic mechanism is rather unlikely, given that both the flavin neutral radical ($FMNH^+$) and the adduct would be formed in a triplet state. Consequently, the adduct spin state would have been detectable in NMR experiments, which was not the case, at least not for the LOV2 domain of *Avena sativa* phototropin [16, 49]. The absence of other intermediate states is corroborated by the concurrence of cysteine deprotonation (τ = 12 µs) and adduct-state formation (τ_{IR} = 18 µs, $\tau_{UV/Vis}$ = 13 µs). These findings exclude an ionic mechanism leaving a photoreaction via radical species as the most plausible scenario, at least for DsLOV-M49S that was studied here.

Materials and Methods

Sample preparation

DsLOV-M49S was heterologously produced and purified as described [30-31].The DsLOV-M49S sample was washed

with 10 mM sodium phosphate buffer at pH 8 by repeated ultrafiltration using Vivaspin 500 filtering devices with 10-kDa cut-off. 1 µL of a 4 mg/mL solution of DsLOV-M49S was placed on a BaF_2 window and dried for 1 h under a gentle stream of nitrogen. The protein film was sealed with a second BaF_2 window and a 1 mm thick spacer. Rehydration was performed through the vapor phase by placing droplets of total volume of 200 µL of a 20% glycerol/water mixture around the protein film as described in [54].

Light-induced FTIR difference spectroscopy

Light-induced FTIR difference spectroscopy was performed on a Vertex 80V spectrometer (Bruker, Rheinstetten, Germany) essentially as described [30]. The hydrated protein sample was kept in the dark for 4 s followed by 3 s of illumination with an LED emitting at a center wavelength of 450 nm (~10 mW/cm²). The temperature was kept constant at 24 °C using a circulating water bath (Julabo F30, Seelbach, Germany). 3,000 light-dark difference spectra were recorded at a spectral resolution of 2 cm^{-1} and averaged.

Flash photolysis in the UV/Vis range

DsLOV-M49S was diluted to a concentration of 60 µM in 10 mM phosphate buffer at pH 8. Absorption changes induced by pulsed laser excitation at 460 nm were recorded across the time range of 50 ns – 10 s on a LKS80 Laser Flash Photolysis Spectrometer (Applied Photophysics). The sample was excited every 20 s and 10 kinetic traces were averaged as described previously [55]. Data were recorded over the wavelength range of 380-730 nm. The 440-500 nm interval was omitted due to scattered light of the exciting laser pulse that hits the detector.

Flash photolysis in the mid-IR range

After pulsed laser excitation (see above), absorption kinetics were recorded in the mid-IR region across the time range of 500 ns - 500 ms with the help of four different tunable external cavity quantum cascade laser (EC-QCL) heads. An EC-QCL with tunable emission across the range of 2600 - 2500 cm^{-1} was used for probing the S-H stretching vibration. The range from 1800 - 1510 cm^{-1} was covered by a series of three tunable EC-QCLs. The sample was excited every 3 s and 100 kinetic traces were recorded at each wavenumber and averaged adapting the procedure described in [38]. A step size of 2 cm^{-1} was chosen for the 1800-1510 cm^{-1} vibrational range and 1 cm^{-1} for the 2600 - 2500 cm^{-1} range. For clarity and to reduce the signal-to-noise ratio after the analysis, spectra were smoothed to yield a spectral resolutions of 4 cm^{-1} (1800-1510 cm^{-1}) and 2 cm^{-1} (2600 - 2500 cm^{-1}), respectively.

ASSOCIATED CONTENT

Table S1, the assignment of the molecular vibrations from Figure 1; Figure S1 Labeled structure of FMN; Figure S2, comparison between time-resolved and steady-state data; Figure S3, the subtraction of heat-induced contamination from the S-H kinetic; Figure S4, Time-resolved UV/vis absorption spectroscopy SAS and concentration profile; Figure S5, Selected kinetics of vibrational bands from the 1800-1510 cm^{-1} range; Figure S6, Lifetime density analysis (LDA); Figure S7, Reaction models used for global target analysis; S8, , kinetics recorded at 1538 cm^{-1} and 2566 cm^{-1}; S9, time-resolved rapid-scan FTIR experiments; Figure S10, Kinetic isotope effect of the triplet decay.

This material is available free of charge via the Internet at http://pubs.acs.org.

AUTHOR INFORMATION

Corresponding Author

* Correspondence: joachim.heberle@fu-berlin.de;

Tel.: +49-30-838-56161

ACKNOWLEDGMENT

R.N.A.M. thanks the Conselho Nacional de Desenvolvimento Científico e Tecnológico – CNPq Brazilian Federal Agency for the scholarship. U.K. acknowledges funding by the Federal Ministry of Education and Research (BMBF) ("OptoSys" project, FKZ 031A16 and FKZ031A167B). This work was supported by the Deutsche Forschungsgemeinschaft through SFB 1078, project B3 to J.H. We thank Aoife Murnin for improving the English style of the text.

ABBREVIATIONS

LOV, Light Oxygen Voltage; DsLOV-M49S, Methionine-to-serine exchange in the LOV protein from *Dinoroseobacter shibae*; FMN, flavin mononucleotide; $[LOV]^3$, triplet state; $[LOV]^A$, FMN cysteinyl-adduct; EC-QCL, external cavity quantum cascade laser.

REFERENCES

1. Christie, J. M., Phototropin blue-light receptors. *Annu Rev Plant Biol* **2007,** *58*, 21-45.
2. Christie, J. M.; Reymond, P.; Powell, G. K.; Bernasconi, P.; Raibekas, A. A.; Liscum, E.; Briggs, W. R., Arabidopsis NPH1: a flavoprotein with the properties of a photoreceptor for phototropism. *Science* **1998,** *282* (5394), 1698-701.
3. Moglich, A.; Yang, X.; Ayers, R. A.; Moffat, K., Structure and function of plant photoreceptors. *Annu Rev Plant Biol* **2010,** *61*, 21-47.
4. Losi, A.; Gardner, K. H.; Moglich, A., Blue-Light Receptors for Optogenetics. *Chem Rev* **2018,** *118* (21), 10659-10709.
5. Gil, A. A.; Laptenok, S. P.; French, J. B.; Iuliano, J. N.; Lukacs, A.; Hall, C. R.; Sazanovich, I. V.; Greetham, G. M.; Bacher, A.; Illarionov, B.; Fischer, M.; Tonge, P. J.; Meech, S. R., Femtosecond to Millisecond Dynamics of Light Induced Allostery in the *Avena sativa* LOV Domain. *J Phys Chem B* **2017,** *121* (5), 1010-1019.
6. Kennis, J. T.; Mathes, T., Molecular eyes: proteins that transform light into biological information. *Interface Focus* **2013,** *3* (5), 20130005.

7. Kennis, J. T.; Crosson, S.; Gauden, M.; van Stokkum, I. H.; Moffat, K.; van Grondelle, R., Primary reactions of the LOV2 domain of phototropin, a plant blue-light photoreceptor. *Biochemistry* **2003,** *42* (12), 3385-92.
8. Swartz, T. E.; Corchnoy, S. B.; Christie, J. M.; Lewis, J. W.; Szundi, I.; Briggs, W. R.; Bogomolni, R. A., The photocycle of a flavin-binding domain of the blue light photoreceptor phototropin. *J Biol Chem* **2001,** *276* (39), 36493-500.
9. Kutta, R. J.; Magerl, K.; Kensy, U.; Dick, B., A search for radical intermediates in the photocycle of LOV domains. *Photochem Photobiol Sci* **2015,** *14* (2), 288-99.
10. Zhu, J.; Mathes, T.; Hontani, Y.; Alexandre, M. T.; Toh, K. C.; Hegemann, P.; Kennis, J. T., Photoadduct Formation from the FMN Singlet Excited State in the LOV2 Domain of Chlamydomonas reinhardtii Phototropin. *J Phys Chem Lett* **2016,** *7* (21), 4380-4384.
11. Alexandre, M. T.; Domratcheva, T.; Bonetti, C.; van Wilderen, L. J.; van Grondelle, R.; Groot, M. L.; Hellingwerf, K. J.; Kennis, J. T., Primary reactions of the LOV2 domain of phototropin studied with ultrafast mid-infrared spectroscopy and quantum chemistry. *Biophys J* **2009,** *97* (1), 227-37.
12. Bednarz, T.; Losi, A.; Gartner, W.; Hegemann, P.; Heberle, J., Functional variations among LOV domains as revealed by FT-IR difference spectroscopy. *Photochem Photobiol Sci* **2004,** *3* (6), 575-9.
13. Dittrich, M.; Freddolino, P. L.; Schulten, K., When light falls in LOV: a quantum mechanical/molecular mechanical study of photoexcitation in Phot-LOV1 of *Chlamydomonas reinhardtii*. *J Phys Chem B* **2005,** *109* (26), 13006-13.
14. Fedorov, R.; Schlichting, I.; Hartmann, E.; Domratcheva, T.; Fuhrmann, M.; Hegemann, P., Crystal structures and molecular mechanism of a light-induced signaling switch: The Phot-LOV1 domain from Chlamydomonas reinhardtii. *Biophys J* **2003,** *84* (4), 2474-82.
15. Crosson, S.; Moffat, K., Structure of a flavin-binding plant photoreceptor domain: insights into light-mediated signal transduction. *Proc Natl Acad Sci U S A* **2001,** *98* (6), 2995-3000.
16. Salomon, M.; Eisenreich, W.; Durr, H.; Schleicher, E.; Knieb, E.; Massey, V.; Rudiger, W.; Muller, F.; Bacher, A.; Richter, G., An optomechanical transducer in the blue light receptor phototropin from Avena sativa. *Proc Natl Acad Sci U S A* **2001,** *98* (22), 12357-61.
17. Christie, J. M.; Swartz, T. E.; Bogomolni, R. A.; Briggs, W. R., Phototropin LOV domains exhibit distinct roles in regulating photoreceptor function. *Plant J* **2002,** *32* (2), 205-19.
18. Avila-Perez, M.; Vreede, J.; Tang, Y.; Bende, O.; Losi, A.; Gartner, W.; Hellingwerf, K., In vivo mutational analysis of YtvA from *Bacillus subtilis*: mechanism of light activation of the general stress response. *J Biol Chem* **2009,** *284* (37), 24958-64.
19. Kottke, T.; Heberle, J.; Hehn, D.; Dick, B.; Hegemann, P., Phot-LOV1: photocycle of a blue-light receptor domain from the green alga Chlamydomonas reinhardtii. *Biophys J* **2003,** *84* (2 Pt 1), 1192-201.
20. Raffelberg, S.; Mansurova, M.; Gartner, W.; Losi, A., Modulation of the photocycle of a LOV domain photoreceptor by the hydrogen-bonding network. *J Am Chem Soc* **2011,** *133* (14), 5346-56.
21. Losi, A.; Gartner, W., The evolution of flavin-binding photoreceptors: an ancient chromophore serving trendy blue-light sensors. *Annu Rev Plant Biol* **2012,** *63*, 49-72.
22. Zayner, J. P.; Sosnick, T. R., Factors that control the chemistry of the LOV domain photocycle. *PLoS One* **2014,** *9* (1), e87074.
23. Magerl, K.; Stambolic, I.; Dick, B., Switching from adduct formation to electron transfer in a light-oxygen-voltage domain containing the reactive cysteine. *Phys Chem Chem Phys* **2017,** *19* (17), 10808-10819.
24. Neiss, C.; Saalfrank, P., Ab initio quantum chemical investigation of the first steps of the photocycle of phototropin: a model study. *Photochem Photobiol* **2003,** *77* (1), 101-9.
25. Zoltowski, B. D.; Schwerdtfeger, C.; Widom, J.; Loros, J. J.; Bilwes, A. M.; Dunlap, J. C.; Crane, B. R., Conformational switching in the fungal light sensor Vivid. *Science* **2007,** *316* (5827), 1054-7.
26. Jentzsch, K.; Wirtz, A.; Circolone, F.; Drepper, T.; Losi, A.; Gartner, W.; Jaeger, K. E.; Krauss, U., Mutual exchange of kinetic properties by extended mutagenesis in two short LOV domain proteins from *Pseudomonas putida*. *Biochemistry* **2009,** *48* (43), 10321-33.
27. Circolone, F.; Granzin, J.; Jentzsch, K.; Drepper, T.; Jaeger, K. E.; Willbold, D.; Krauss, U.; Batra-Safferling, R., Structural basis for the slow dark recovery of a full-length LOV protein from *Pseudomonas putida*. *J Mol Biol* **2012,** *417* (4), 362-74.
28. Metz, S.; Jager, A.; Klug, G., Role of a short light, oxygen, voltage (LOV) domain protein in blue light- and singlet oxygen-dependent gene regulation in *Rhodobacter sphaeroides*. *Microbiology (Reading)* **2012,** *158* (Pt 2), 368-379.
29. Swartz, T. E.; Wenzel, P. J.; Corchnoy, S. B.; Briggs, W. R.; Bogomolni, R. A., Vibration spectroscopy reveals light-induced chromophore and protein structural changes in the LOV2 domain of the plant blue-light receptor phototropin 1. *Biochemistry* **2002,** *41* (23), 7183-9.
30. Endres, S.; Granzin, J.; Circolone, F.; Stadler, A.; Krauss, U.; Drepper, T.; Svensson, V.; Knieps-Grunhagen, E.; Wirtz, A.; Cousin, A.; Tielen, P.; Willbold, D.; Jaeger, K. E.; Batra-Safferling, R., Structure and function of a short LOV protein from the marine phototrophic bacterium *Dinoroseobacter shibae*. *BMC Microbiol* **2015,** *15*, 30.
31. Fettweiss, T.; Rollen, K.; Granzin, J.; Reiners, O.; Endres, S.; Drepper, T.; Willbold, D.; Jaeger, K. E.; Batra-Safferling, R.; Krauss, U., Mechanistic Basis of the Fast Dark Recovery of the Short LOV Protein DsLOV from *Dinoroseobacter shibae*. *Biochemistry* **2018,** *57* (32), 4833-4847.
32. Ataka, K.; Hegemann, P.; Heberle, J., Vibrational spectroscopy of an algal Phot-LOV1 domain probes the molecular changes associated with blue-light reception. *Biophys J* **2003,** *84* (1), 466-74.
33. Kerruth, S.; Langner, P.; Raffelberg, S.; Gartner, W.; Heberle, J., Characterization of the Blue-Light-Activated Adenylyl Cyclase mPAC by Flash Photolysis and FTIR Spectroscopy. *Photochem Photobiol* **2017,** *93* (3), 857-864.
34. Iwata, T.; Nozaki, D.; Sato, Y.; Sato, K.; Nishina, Y.; Shiga, K.; Tokutomi, S.; Kandori, H., Identification of the C=O Stretching Vibrations of FMN and Peptide Backbone by ^{13}C-Labeling of the LOV2 Domain of *Adiantum* Phytochrome3. *Biochemistry* **2006,** *45* (51), 15384-15391.
35. Pfeifer, A.; Majerus, T.; Zikihara, K.; Matsuoka, D.; Tokutomi, S.; Heberle, J.; Kottke, T., Time-resolved Fourier transform infrared study on photoadduct formation and secondary structural changes within the phototropin LOV domain. *Biophys J* **2009,** *96* (4), 1462-70.
36. Konold, P. E.; Mathes, T.; Weibetaenborn, J.; Groot, M. L.; Hegemann, P.; Kennis, J. T., Unfolding of the C-Terminal Jalpha Helix in the LOV2 Photoreceptor Domain Observed by Time-Resolved Vibrational Spectroscopy. *J Phys Chem Lett* **2016,** *7* (17), 3472-6.
37. Halavaty, A. S.; Moffat, K., N- and C-terminal flanking regions modulate light-induced signal transduction in the LOV2 domain of the blue light sensor phototropin 1 from Avena sativa. *Biochemistry* **2007,** *46* (49), 14001-9.
38. Schultz, B. J.; Mohrmann, H.; Lorenz-Fonfria, V. A.; Heberle, J., Protein dynamics observed by tunable mid-IR quantum cascade lasers across the time range from 10ns to 1s. *Spectrochim Acta A Mol Biomol Spectrosc* **2018,** *188*, 666-674.
39. Bare, G. H.; Alben, J. O.; Bromberg, P. A., Sulfhydryl groups in hemoglobin. A new molecular probe at the alpha1 beta 1 interface studied by Fourier transform infrared spectroscopy. *Biochemistry* **1975,** *14* (8), 1578-83.
40. Iwata, T.; Tokutomi, S.; Kandori, H., Photoreaction of the cysteine S-H group in the LOV2 domain of Adiantum phytochrome3. *J Am Chem Soc* **2002,** *124* (40), 11840-1.
41. Song, S. H.; Freddolino, P. L.; Nash, A. I.; Carroll, E. C.; Schulten, K.; Gardner, K. H.; Larsen, D. S., Modulating LOV domain

photodynamics with a residue alteration outside the chromophore binding site. *Biochemistry* **2011,** *50* (13), 2411-23.
42. Martin, C. B.; Tsao, M. L.; Hadad, C. M.; Platz, M. S., The reaction of triplet flavin with indole. A study of the cascade of reactive intermediates using density functional theory and time resolved infrared spectroscopy. *J Am Chem Soc* **2002,** *124* (24), 7226-34.
43. Thoing, C.; Pfeifer, A.; Kakorin, S.; Kottke, T., Protonated triplet-excited flavin resolved by step-scan FTIR spectroscopy: implications for photosensory LOV domains. *Phys Chem Chem Phys* **2013,** *15* (16), 5916-26.
44. Iuliano, J. N.; Gil, A. A.; Laptenok, S. P.; Hall, C. R.; Tolentino Collado, J.; Lukacs, A.; Hag Ahmed, S. A.; Abyad, J.; Daryaee, T.; Greetham, G. M.; Sazanovich, I. V.; Illarionov, B.; Bacher, A.; Fischer, M.; Towrie, M.; French, J. B.; Meech, S. R.; Tonge, P. J., Variation in LOV Photoreceptor Activation Dynamics Probed by Time-Resolved Infrared Spectroscopy. *Biochemistry* **2018,** *57* (5), 620-630.
45. Freddolino, P. L.; Dittrich, M.; Schulten, K., Dynamic switching mechanisms in LOV1 and LOV2 domains of plant phototropins. *Biophys J* **2006,** *91* (10), 3630-9.
46. Zayner, J. P.; Antoniou, C.; Sosnick, T. R., The amino-terminal helix modulates light-activated conformational changes in AsLOV2. *J Mol Biol* **2012,** *419* (1-2), 61-74.
47. Domratcheva, T.; Fedorov, R.; Schlichting, I., Analysis of the Primary Photocycle Reactions Occurring in the Light, Oxygen, and Voltage Blue-Light Receptor by Multiconfigurational Quantum-Chemical Methods. *J Chem Theory Comput* **2006,** *2* (6), 1565-74.
48. Schleicher, E.; Kowalczyk, R. M.; Kay, C. W.; Hegemann, P.; Bacher, A.; Fischer, M.; Bittl, R.; Richter, G.; Weber, S., On the reaction mechanism of adduct formation in LOV domains of the plant blue-light receptor phototropin. *J Am Chem Soc* **2004,** *126* (35), 11067-76.
49. Kay, C. W.; Schleicher, E.; Kuppig, A.; Hofner, H.; Rudiger, W.; Schleicher, M.; Fischer, M.; Bacher, A.; Weber, S.; Richter, G., Blue light perception in plants. Detection and characterization of a light-induced neutral flavin radical in a C450A mutant of phototropin. *J Biol Chem* **2003,** *278* (13), 10973-82.
50. Nakagawa, S.; Weingart, O.; Marian, C. M., Dual Photochemical Reaction Pathway in Flavin-Based Photoreceptor LOV Domain: A Combined Quantum-Mechanics/Molecular-Mechanics Investigation. *J Phys Chem B* **2017,** *121* (41), 9583-9596.
51. Bauer, C.; Rabl, C. R.; Heberle, J.; Kottke, T., Indication for a radical intermediate preceding the signaling state in the LOV domain photocycle. *Photochem Photobiol* **2011,** *87* (3), 548-53.
52. Kottke, T.; Dick, B.; Fedorov, R.; Schlichting, I.; Deutzmann, R.; Hegemann, P., Irreversible photoreduction of flavin in a mutated Phot-LOV1 domain. *Biochemistry* **2003,** *42* (33), 9854-9862.
53. Bittl, R.; Kay, C. W.; Weber, S.; Hegemann, P., Characterization of a flavin radical product in a C57M mutant of a LOV1 domain by electron paramagnetic resonance. *Biochemistry* **2003,** *42* (28), 8506-12.
54. Lorenz-Fonfria, V. A.; Heberle, J., Proton transfer and protein conformation dynamics in photosensitive proteins by time-resolved step-scan Fourier-transform infrared spectroscopy. *J Vis Exp* **2014,** (88), e51622.
55. Kerruth, S.; Ataka, K.; Frey, D.; Schlichting, I.; Heberle, J., Aureochrome 1 illuminated: structural changes of a transcription factor probed by molecular spectroscopy. *PLoS ONE* **2014,** *9* (7), e103307.